Arch. Metall. Mater., Vol. 61 (2016), No 2, p. 629–634

DOI: 10.1515/amm-2016-0107

YEONG-JU CHOE*, KYOUNG-JIN LEE*, HAE-JIN HWANG*# **

Cr POISONING ON $Nd_2Ni_{0.95}Cu_{0.05}O_{4+\delta}$ CATHODE FOR SOLID OXIDE FUEL CELLS

In this study, $Nd_2Ni_{1-x}Cu_xO_{4+\delta}$ (x=0, 0.05, 0.1, and 0.2) layered perovskite powders were synthesized by the glycine nitrate process (GNP) and the chromium poisoning effect on the electrochemical performance of the $Nd_2Ni_{0.95}Cu_{0.05}O_{4+\delta}$ and $La_{0.6}Sr_{0.4}Co_{0.2}Fe_{0.8}O_{3-\delta}$ cathodes were investigated. In the case of the LSCF cathode, the strontium chromite phase formed after the exposure of the gaseous chromium species, while there was no additional phase in the $Nd_2Ni_{0.95}Cu_{0.05}O_{4+\delta}$ cathode. The area specific resistance (ASR) of the $Nd_2Ni_{0.95}Cu_{0.05}O_{4+\delta}$ cathode did not change significantly after the exposure of the gaseous chromium species at 800°C.

Keywords: chromium poisoning, layered perovskite, Ruddlesden-Popper, solid oxide fuel cells, Nd2NiO4

1. Introduction

A solid oxide fuel cell (SOFC) is an electrochemical conversion device that produces electricity directly from fuel (hydrogen) and oxidant (oxygen or air). From the point of efficiency, the SOFC system are more efficient when it is operated in the temperature range of 850~1000°C [1-3]. However, in order to enhance the long-term durability of the stack and reduce the overall system cost, lowering the operating temperature of the SOFC system to the intermediate temperature range (650-850°C) has been one of the most important research issues in the past few decades [4].

The intermediate temperature SOFC (IT-SOFC) consists of a dense stabilized zirconia, typically yttria- or scandia-stabilized zirconia (YSZ or ScSZ), porous cathode and Ni-YSZ cermet anode. The cathode is mostly strontium- and cobalt-doped lanthanum ferrite (LSCF), which show good catalytic activity, mixed electronic and ion conductivity, and compatible thermal expansion coefficient with the zirconia- or ceria-based electrolytes [5-7]. However, the LSCF cathode suffers from the interfacial instability problem, which results from the strontium diffusion across the ceria (CeO_2) buffer layer between the LSCF cathode and YSZ electrolyte and the poisoning of the cathode by volatile chromium species from the ferritic stainless steel-based interconnects [8-10].

Some Ruddlesden-Popper (RP) type layered perovskites with the general formula of $A_{1+n}B_nO_{3n+1}$, where A and B are cations, possess interesting properties such as superconductivity, magneto-resistance and catalytic activity for oxygen reduction reaction (ORR). In addition, owing to the layered structure of the RP perovskite, the oxygen located in between the two perovskite layers can be easily moved, which allows it to be a good oxygen ion conductor in the intermediate temperature range. In this regard, there has been increasing interest in utilizing the RP type perovskites as an alternative to the state-of-the-art LSCF cathode, oxygen separators, oxygen sensors and so on [11,12].

Among various RP type layered perovskites, it has been known that the undoped Nd2NiO4+δ showed better ionic conductivity and catalytic activity than the doped ones since the substitution for neodymium or nickel can lead to reduce the oxygen overstoichiometry [13]. In this study, a copper doped neodymium nickelate, $Nd_2Ni_{1-x}Cu_xO_{4+\delta}$ (x=0, 0.05, 0.1, and 0.2) layered perovskites powder was fabricated by the glycine nitrate process (GNP) and the chromium poisoning effect on the electrochemical performance of the $Nd_2Ni_{1-x}Cu_xO_{4+\delta}$ cathode was investigated in terms of the copper doing content and temperatures [14-16].

2. Experimental

Three powder samples with the composition of $Nd_2Ni_{1-x}Cu_xO_{4+\delta}$ (x=0, 0.05, 0.1, and 0.2) were synthesized by the glycine-nitrate process. The flowchart for preparation of the powder was shown in Fig. 1 (a). Starting materials are $Nd(NO_3)_3 \cdot 6H_2O$ (99.9%, Sigma-Aldrich, USA), $Ni(NO_3)_2 \cdot 6H_2O$ (99.9%, Sigma-Aldrich, USA), $Cu(NO_3)_2 \cdot xH_2O$ (99.99%, Sigma-Aldrich, USA) and glycine (99.0%, Junsei, Japan). The metal nitrates were dissolved in distilled water and then the glycine was added into the mixed nitrate solution in a molar ratio of 2:1 for fuel: metal ions. At x=0, a molar ratio is exceptively 1:1. The mixture is heated up 200°C. After the combustion reaction, the as-synthesized powder was calcined at 1000°C for 5 h.

Symmetrical cells of $Nd_2Ni_{1-x}Cu_xO_{4+\delta}$/GDC(gadolinium-doped ceria, $Ce^{0.9}Gd_{0.1}O$, Anan Kasei, Japan)/$Nd_2Ni_{1-x}Cu_xO_{4+\delta}$ configuration was fabricated by screen-printing the $Nd_2Ni_{1-x}Cu_xO_{4+\delta}$ inks on the both sides of a GDC disk and subsequently

* DEPARTMENT OF MATERIALS SCIENCE AND ENGINEERING, INHA UNIVERSITY, INCHEON, KOREA

Corresponding author: hjhwang@inha.ac.kr

calcined at 1000°C for 2 h in air. For comparison, a symmetrical cell of LSCF/GDC/LSCF configuration was also prepared in the same method using a $La_{0.6}Sr_{0.4}Co_{0.2}Fe_{0.8}O_{3-\delta}$ (Fuel Cell Materials, USA) powder. For the chromium poisoning of the cathode, the cells were heat-treated at 800°C for 100 h in the atmosphere of gaseous chromium species that was produced by chromium oxide (Cr_2O_3) powder compact as shown in Fig. 1 (b). The Cr_2O_3 powder compact was prepared from a commercially available Cr_2O_3 powder (99.0%, Junsei, Japan). The powder was dry-pressed into a disk and sintered at 1000°C for 1 h. In order to clarify the effect of the gaseous chromium species on the cathode performance, the cells were also heat-treated at 800°C for 100 h in air.

Phase identification of the synthesized powder was performed with a powder diffractometer (DMAX-2500, Rigaku, Japan) with Ni-filtered Cu Kα radiation. The microstructure of the cathode was observed by field emission scanning electron microscope (FE-SEM, S-3200, Philips).

The electrochemical performance of the symmetrical cells was measured by electrochemical impedance spectroscopy (EIS). AC impedance spectroscopy was performed, with an excitation potential of 20mV, over a frequency range from 1 MHz to 0.1 Hz, generated by a frequency analyzer (IM6e, Zhaner).

Rectangular bar samples were prepared from GDC and $Nd_2Ni_{0.95}Cu_{0.05}O_{4+\delta}$ powders for the measurement of the electrical conductivity. The GDC powder was pressed uniaxially, followed by cold isostatic pressing (CIP) at 200 MPa. The CIPed bar samples were sintered at 1450°C for 5 h in air. The inks of $Nd_2Ni_{0.95}Cu_{0.05}O_{4+\delta}$ and LSCF were screen-printed on one side of the GDC bar sample and then heat-treated at 1000°C for 2 h in air as shown in Fig. 1 (c). The electrical conductivity was measured at 800°C for 40 h in the atmosphere of gaseous chromium species by the DC-four probe method using a high accuracy multimeter (Medel 2400, Keithley Instruments Inc.).

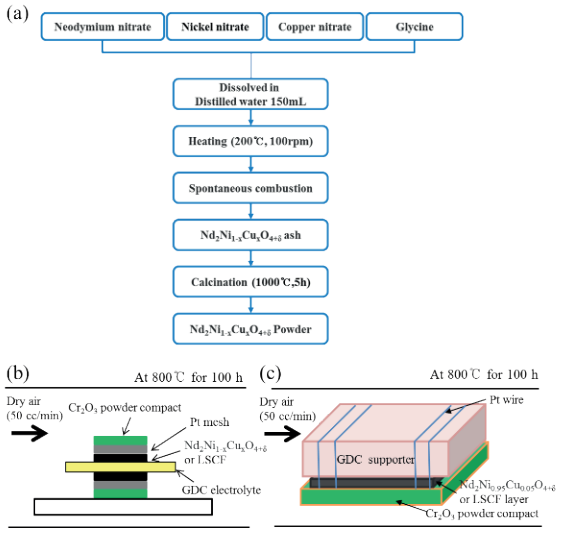

Fig. 1. Schematic diagram for the synthesis of the $Nd_2Ni_{1-x}Cu_xO_{4+\delta}$ powders (a), the Cr-poisoning experimental (b), and the schematic figure of the samples for conductivity measurement in the gaseous chromium species.

3. Results and discussion

Fig. 2 shows XRD patterns of $Nd_2Ni_{1-x}Cu_xO_{4+\delta}$ powders calcined at 1000°C for 5 h in air. Reflections corresponding to the identified phases are labeled and closely match with JCPDS data (File No. 01-088-0761). It can be seen that the synthesized powders are identified as a single-phase layered perovskite of general formula of $A_2BO_{4+\delta}$[15].

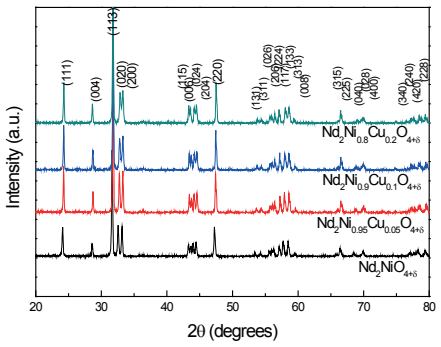

Fig. 2. XRD patterns of the synthesized $Nd_2Ni_{1-x}Cu_xO_{4+\delta}$ (x=0, 0.05, 0.1, 0.2) powder calcined at 1000°C

Fig. 3 shows cross-sectional SEM images for the $Nd_2Ni_{0.95}Cu_{0.05}O_{4+\delta}$ and LSCF cathodes after being sintered at 1000°C for 2 h in the symmetrical cell. The cathodes have a porous microstructure and 35 μm and 18 μm thickness, respectively. The cathode adhered well to electrolyte surface and the electrolyte is dense without cracks or pores [17].

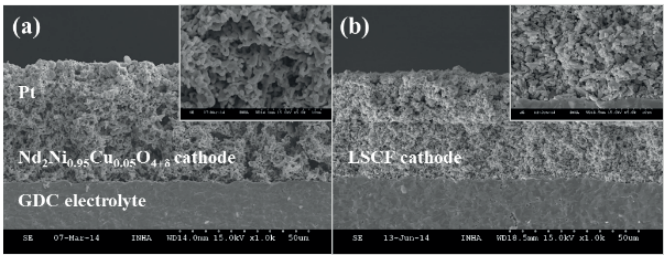

Fig. 3. Cross-sectional SEM images of $Nd_2Ni_{0.95}Cu_{0.05}O_{4+\delta}$/GDC/$Nd_2Ni_{0.95}Cu_{0.05}O_{4+\delta}$ and LSCF/GDC/LSCF symmetric cells

Fig. 4 (a) and Table 1 presents the ASR values of the symmetric cells with $Nd_2Ni_{1-x}Cu_xO_{4+\delta}$ (x=0, 0.05, 0.1, 0.2) as a function of temperature. The lowest ASR value was obtained at x=0.05 sample and the ASR was increased with increasing copper contents. It appears that there are two opposed effect of the copper addition on the catalytic activity of the $Nd_2NiO_{4+\delta}$ oxygen ion conductivity increases with increasing copper content, while electrical conductivity increases with decreasing copper content. Thus, adding small amount of copper is the trade-off in two properties and as a consequence, the cathode sample with x=0.05 exhibited the lowest ASR value [26,27].

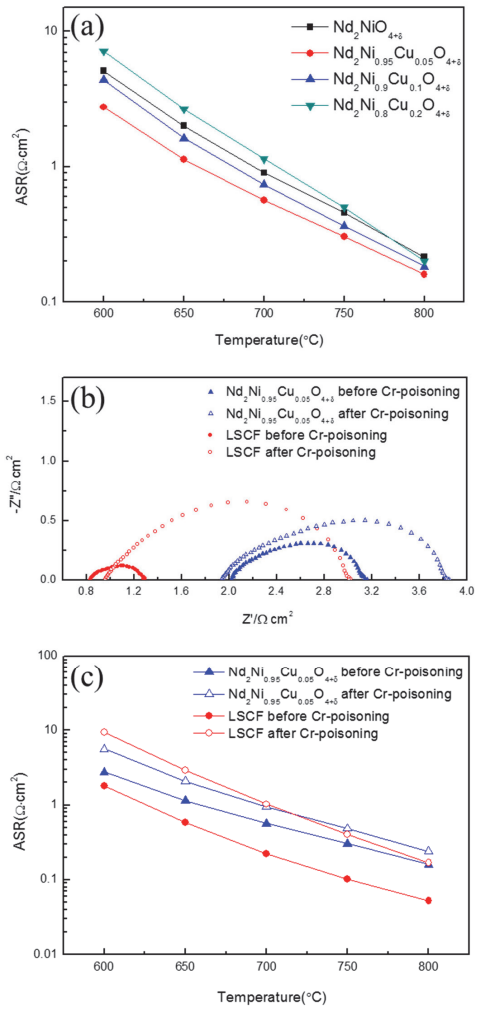

Fig. 4. Arrhenius plots of the ASRs of the $Nd_2Ni_{1-x}Cu_xO_{4+\delta}$ (x=0, 0.05, 0.1, 0.2) cathodes (a), AC Impedance spectra of the $Nd_2Ni_{0.95}Cu_{0.05}O_{4+\delta}$ and LSCF cathodes measured at 700°C (b) and Arrhenius plots of the ASRs of the $Nd_2Ni_{0.95}Cu_{0.05}O_{4+\delta}$ and LSCF cathodes.

Fig. 4 (b) shows the AC impedance spectra of the symmetric cells with $Nd_2Ni_{0.95}Cu_{0.05}O_{4+\delta}$ and LSCF cathode on GDC electrolyte at 700°C before and after Cr-poisoning. The ASR values as a function of temperature are shown in Fig. 4 (c) and Table 2. Polarization resistance Rp derived from difference between Rt and Ro (Rp = Rt–Ro or area specific resistance, ASR). It means the overall cathodic properties related with the oxygen reduction, oxygen surface/bulk diffusion and the gas phase oxygen diffusion [18].

After Cr-poisoning, the ASR of LSCF cathode was significantly increased by a factor of 4.5 to 1.0255 Ω.cm², whereas that of $Nd_2Ni_{0.95}Cu_{0.05}O_{4+\delta}$ cathode was increased 1.7 times to 0.95 Ω.cm² at 700°C. In addition, the ASR of $Nd_2Ni_{0.95}Cu_{0.05}O_{4+\delta}$ cathode was lower than that of LSCF cathode below 700°C. Finsterbusch et al. [19] studied that the chromium oxide coating on LSCF can result in the drastic decrease in the effective surface exchange coefficients kchem, which is considered to be responsible for the drastic increase in the ASR value of the LSCF cathode. Yang et al. [20] addressed that the kchem of $Nd_2NiO_{4+\delta}$ with 30 nm Cr was slightly decreased from the level of the sample without Cr-layer for 1000 h at 600°C. In the nickelate, Ni is enriched, while Nd is depleted in the Cr-rich surface zone [20-22], which may has a minor effect on k_{chem}, and the increase in the ASR of $Nd_2Ni_{0.95}Cu_{0.05}O_{4+\delta}$. However, the effect on the cathode performance was reported to be negligible.

Porous LSCF and $Nd_2Ni_{0.95}Cu_{0.05}O_{4+\delta}$ layers on dense GDC bars were prepared for electrical conductivity measurements shown in Fig. 5 (a) and (b). The open porosity enabled vapor phase transport of volatile Cr-species into the $Nd_2Ni_{0.95}Cu_{0.05}O_{4+\delta}$ or LSCF layer [22]. A surface area of coated layers is 6.0 mm x 3.5 mm and thickness of those is about 15 μm.

Fig. 5 indicates the electrical conductivity evolution with time of the $Nd_2Ni_{0.95}Cu_{0.05}O_{4+\delta}$ and LSCF at 800°C under air and atmosphere of gaseous chromium species. Conductivity of the LSCF sample was gradually decreased as a function

TABLE 1

Polarization resistances (Ω.Cm²) of the $Nd_2Ni_{1-x}CuxO_{4+\delta}$ cathodes.

Temperature	Rp(Ω.Cm²)			
	$Nd_2NiO_{4+\delta}$	$Nd_2Ni_{0.95}Cu_{0.05}O_{4+\delta}$	$Nd_2Ni_{0.9}Cu_{0.1}O_{4+\delta}$	$Nd_2Ni_{0.8}Cu_{0.2O4+\delta}$
600°C	5.1	2.755	4.38	7.15
650°C	2.005	1.135	1.625	2.675
700°C	0.9	0.565	0.74	1.14
750°C	0.455	0.305	0.365	0.5
800°C	0.215	0.16	0.183	0.2

TABLE 2

Polarization resistances (Ω.Cm²) of the $Nd_2Ni_{0.95}Cu_{0.05}O_{4+\delta}$ and LSCF cathodes before and after Cr-poisoning

Temperature	Rp(Ω.Cm²)			
	$Nd_2Ni_{0.95}Cu_{0.05}O_{4+\delta}$		LSCF	
	Before Cr-poisoning	After Cr-poisoning	Before Cr-poisoning	After Cr-poisoning
600°C	2.755	5.625	1.785	9.385
650°C	1.135	2.08	0.58	2.915
700°C	0.565	0.95	0.2235	1.0255
750°C	0.305	0.485	0.1025	0.405
800°C	0.16	0.24	0.052	0.1685

of time especially in the gaseous chromium atmosphere. On the other hand, conductivity of the $Nd_2Ni_{0.95}Cu_{0.05}O_{4+\delta}$ sample was almost constant as a function of time both in air and the gaseous chromium atmosphere.

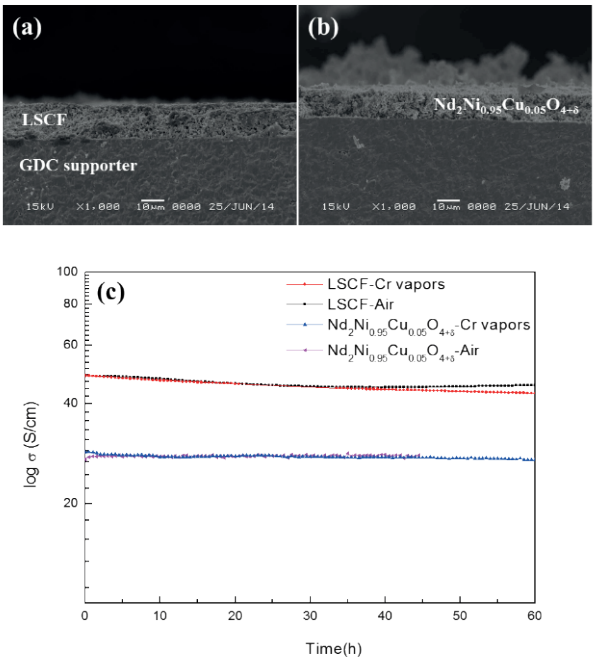

Fig. 5. Electrical conductivity as a function of time of the $Nd_2Ni_{0.95}Cu_{0.05}O_{4+\delta}$ and LSCF samples in the gaseous chromium species at 800°C

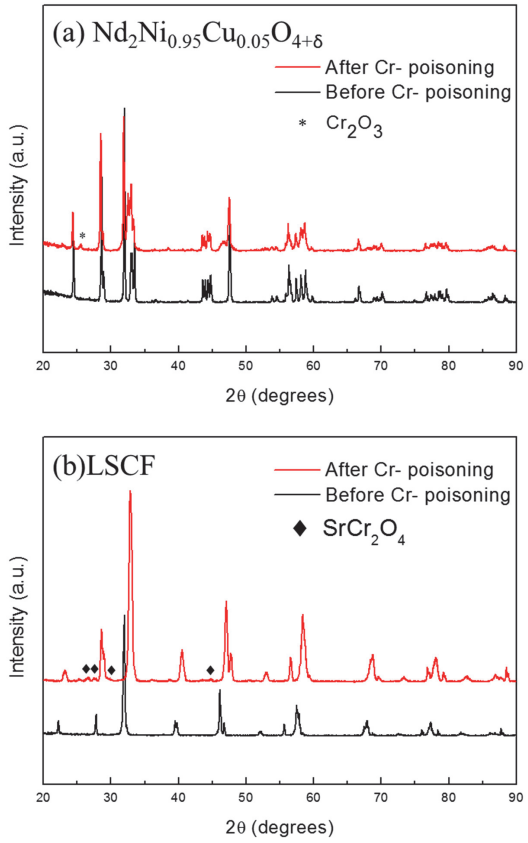

Fig. 6. XRD patterns of the $Nd_2Ni_{0.95}Cu_{0.05}O_{4+\delta}$ (a) and LSCF cathode (b) before and after Cr-poisoning experimental

XRD patterns of $Nd_2Ni_{0.95}Cu_{0.05}O_{4+\delta}$ and LSCF cathode before and after Cr-poisoning were shown in Fig. 6. The formation of strontium chromite ($SrCr_2O_4$) was confirmed in the case of the LSCF cathode after Cr-poisoning as can be seen in Fig. 6 (b). It seems that the strontium in the LSCF cathode reacts with the gaseous chromium species to produce the strontium chromite crystal phases during the exposure to volatile Cr-species, which probably causes the observed degradation [23-24]. In case of $Nd_2Ni_{0.95}Cu_{0.05}O_{4+\delta}$ cathode, no additional peaks were observed after Cr-poisoning. Although some peaks which corresponds to the chromium oxide (Cr_2O_3) phase was detected, this is associated with the chromium oxide (Cr_2O_3) powder compact.

4. Conclusions

Single phase $Nd_2Ni_{1-x}Cu_xO_{4+\delta}$ (x=0.05, 0.1, and 0.2) layered perovskite powders were synthesized by the glycine nitrate process (GNP). Although the area specific resistance (ASR) of the $Nd_2Ni_{0.95}Cu_{0.05}O_{4+\delta}$ cathode was slightly higher than that of the LSCF cathode, the increase in the ASR value after the chromium poisoning was more significant in the LSCF cathode than the $Nd_2Ni_{0.95}Cu_{0.05}O_{4+\delta}$ cathode. The conductivity change as a function of time under the gaseous chromium species was also modest in the $Nd_2Ni_{0.95}Cu_{0.05}O_{4+\delta}$ cathode. There, it could be concluded that the $Nd_2Ni_{0.95}Cu_{0.05}O_{4+\delta}$ cathode was tough against the chromium poisoning. The observed chromium poisoning in the LSCF cathode resulted from the formation of the strontium chromite phase in the LSCF cathode.

Acknowledgments

This work was supported by the New & Renewable Energy Core Technology Program of the Korea Institute of Energy Technology Evaluation and Planning (KETEP), granted financial resource from the Ministry of Trade, Industry & Energy, Republic of Korea. (No. 20113020030050)

This work was supported by the Fundamental R&D Program for Core Technology of Materials (No.10051006) of the Korea Evaluation Institute of Industrial Technology (KEIT), Republic of Korea.

REFERENCES

[1] J. Huijsmans, F. Van Berkel, G. Christie, J.Power Sources. **71**, 107-110 (1998).
[2] N.Q. Minh, Solid State Ionics. **174**, 271-277 (2004).
[3] C. Lalanne, F. Mauvy, E. Siebert, M. Fontaine, J. Bassat, F .Ansart, et al, Journal of the European Ceramic Society. **27**, 4195-4198 (2007).
[4] J.M. Ralph, C. Rossignol, R. Kumar, J.Electrochem Soc. **150**, A1518-A1522 (2003).
[5] A. Atkinson, S. Barnett, R.J. Gorte, J. Irvine, A.J. McEvoy, M Mogensen, et al, Nature materials. **3**, 17-27 (2004).
[6] H. Zhao, F. Mauvy, C. Lalann, J. Bassat, S. Fourcade, J. Grenier, Solid State Ionics. **179**, 2000-2005 (2008).
[7] K. Murata, T. Fukui, H. Abe, M. Naito, K. Nogi, J.Power

Sources. **145**, 257-261 (2005).
[8] S.P. Jiang, S. Zhang, Y. Zhen, J.Electrochem.Soc. **153**, A127-A134 (2006).
[9] B. Fan, J. Yan, X. Yan, Solid State Sciences. **13**, 1835-1839 (2011).
[10] M.C. Tucker, H. Kurokawa, C.P. Jacobson, L.C De Jonghe, SJ Visco, J.Power Sources. **160**, 130-138 (2006).
[11] Y. Wang, H. Nie, S. Wang, T. Wen, U. Guth, V. Valshook, Mater Lett. **60**, 1174-1178 (2006).
[12] V.V. Kharton, A.V. Kovalevsky, M. Avdeev, E.V. Tsipis, M.V. Patrakeev, A.A. Yaremchenko, et al, Chemistry of materials. **19**, 2027-2033 (2007).
[13] A. Egger, W. Sitte, F. Klauser, E. Bertel, J.Electrochem Soc. **157**, B1537-B1541 (2010).
[14] L.A. Chick, L. Pederson, G. Maupin, J. Bates, L. Thomas, G. Exarhos, Mater Lett 10 6-12 (1990).
[15] M. Soorie, S.J. Skinner, Solid State Ionics. **177**, 2081-2086 (2006).
[16] J. Kim, E. Kvam, Physica C: Superconductivity. **292**, 203-210 (1997).
[17] F. Meng, T. Xia, J. Wang, Z. Shi, J. Lian, H. Zhao, et al, Int J Hydrogen Energy. **39**, 4531-4543 (2014).
[18] B. Wang, G. Long, Y. Ji, M. Pang, X. Meng, J.Alloys Compounds. **606**, 92-96 (2014).
[19] M Finsterbusch, A Lussier, E Negusse, Z Zhu, RJ Smith, JA Schaefer, et al, Solid State Ionics. 181, **640-645** (2010).
[20] M. Yang, E. Bucher, W. Sitte, J.Power Sources. **196**, 7313-7317 (2011).
[21] J. Andreas Schuler, H. Lübbe, A. Hessler-Wyser, J. Van herle, J.Power Sources. **213**, 223-228 (2012).
[22] M.K. Stodolny, B.A. Boukamp, DHA Blank, FPF van Berkel, J.Power Sources. **196**, 9290-9298 (2011).
[23] G.Y. Lau, M.C. Tucker, C.P .Jacobson, S.J. Visco, S.H. Gleixner, L.C. DeJonghe, J.Power Sources. **195**, 7540-7547 (2010).
[24] S.P. Jiang, X. Chen, Int J Hydrogen Energy. 39, 505-531 (2014).
[25] E. Konysheva, H. Penkalla, E. Wessel, J. Mertens, U. Seeling, L. Singheiser, et al, J.Electrochem Soc. **153**, A765-A773 (2006).
[26] A. Khandale, S. Bhoga, R. Kumar, Solid State Ionics. **238**, 1-6 (2013).
[27] A. Aguadero, J. Alonso, M. Escudero, L. Daza, Solid State Ionics. **179**, 393-400 (2008).